Pure appl. geophys. 161 (2004) 93–122
0033 – 4553/04/010093 – 30
DOI 10.1007/s00024-003-2431-z

Pure and Applied Geophysics

Interrelationships Between Topography, Quaternary Vertical Displacement, Active Faults and Short-term Horizontal Crustal Strain in Honshu, Japan

Thomas H. Wilson,[1] Kazuhiko Kano,[2] and Osamu Nishizawa[2]

Abstract—Regional and local characteristics of active fault patterns and elevation variation throughout Honshu, Japan are characterized in terms of their fractal dimensions; this allows variation in these complex variables to be compared directly to the scalar properties of net Quaternary vertical displacement, elevation and 10- and 110-year horizontal strains.

The comparisons reveal that, throughout Honshu as a whole, there is significant correlation ($\langle r \rangle = 0.75$) between Quaternary vertical displacement, elevation, and its fractal properties. There is poor correlation, however, of elevation and its fractal properties to horizontal crustal strain, and also between Quaternary vertical displacement and horizontal crustal strain. A slight negative correlation is observed between the fractal properties of the active fault system and horizontal crustal strain measured over 10- and 110-year time periods (−0.43 and −0.26, respectively). The correlation between the 10-year (1985–1994) and 110-year (1883–1994) area strains, 0.48, reveals the occurrence of considerable change in the distribution of regional strain over these short time frames.

Local computations of the correlation between data sets made for overlapping 160 km length windows of data spaced every 20 km along analysis lines reveal internal fluctuations in the correlation between variables. The local correlation between Quaternary vertical displacement and elevation is highest through central Japan and the Kinki Triangle. There is weak negative correlation between area strain and fractal dimensions of the active fault network. The local correlation between the fractal dimensions of active faults and horizontal area strain over the recent 10-year time period averages about −0.6 through central Japan in an area that extends across the Kinki Triangle through the northern part of central Honshu and northeast across the Itoigawa Shizuoka Tectonic Line. In general, regions of greatest complexity in the active fault network are associated with persistent negative area or compressional strain. Sparsely faulted areas in general coincide with areas of positive or roughly zero area strain. The presence of negative correlation through central Japan and the Kinki Triangle area in the recent 10-year period results from a decrease of area strain within an increasingly complex active fault system that reaches maximum negative values concentrated in the Kinki Triangle during the 1985–1994 time period.

Key words: Fractals, complexity, topography, active faults, Quaternary vertical displacement, crustal strain, Japan.

[1] Department of Geology and Geography, West Virginia University, Morgantown, West Virginia.
E-mail: wilson@geo.wvu.edu

[2] Geological Survey of Japan, Tsukuba, Japan.
E-mail: osamu-nishizawa@aist.go.jp and kazu.kano@aist.go.jp

1. Introduction

Quantitative comparisons between fractal properties of topography and active fault patterns with elevation, Quaternary vertical displacement, and short-term horizontal crustal strain measured over recent 10- and 110-year time intervals are undertaken in Honshu, Japan. Data comparisons are made along three analysis lines that run the length of Honshu. Some of the major tectonic elements and boundaries referenced in the following discussions are shown in Figure 1.

Analyses of topography in other parts of the world (e.g., MARK and ARONSON, 1984; MALINVERNO, 1990; KLINKENBERG and GOODCHILD, 1992; WILSON and DOMINIC, 1998; DOUDS, 1998) reveal that topography has fractal properties. Tectonic processes partly determine the fractal characteristics of topography in many locations. WILSON and DOMINIC (1998), for example, found an average correlation of 0.71 between the fractal dimensions of surface topography and structural relief measured along 24 profiles through a portion of the central Appalachian Valley and Ridge province in eastern North America. In the less-

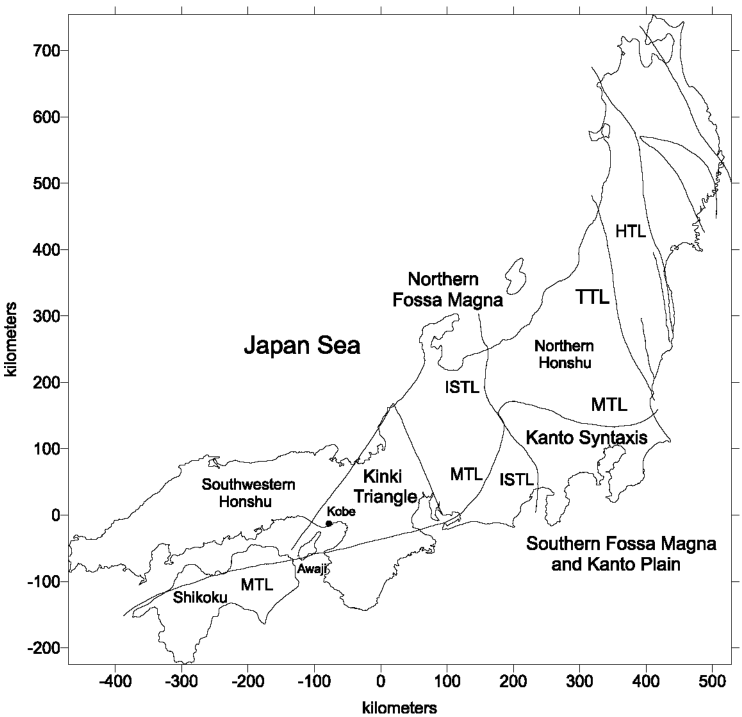

Figure 1
Reference map shows major faults and tectonic boundaries in Honshu. MTL—Median Tectonic Line; ISTL—Itoigawa-Shizuoka Tectonic Line; TTL—Tanakura Tectonic Line; HTL—Hategawa Tectonic Line.

deformed Appalachian Plateau province they found that the fractal dimension of surface topography remains constant and is similar in value to the fractal dimension of near-surface structure calculated from shallow seismic reflection events. Fractal analysis of topography in a roughly 100,000 km^2 region of the central Appalachians conducted by DOUDS (1998) revealed associations between variations in the fractal dimension of topography and major tectonic subdivisions of the Appalachian foreland fold and thrust belt.

The earth's surface topography and its variation from one place to another is the net result of constructive physical processes such as plate tectonic interaction, volcanic eruptions and sedimentation, and degradational processes such as chemical and mechanical weathering, erosion and subsidence. The variable mechanical and chemical properties of geologic formations allow weathering to proceed at a variable pace and thus expose the outlines of near-surface structures. The structural imprint on surface topography is often vividly displayed in aerial photographs and satellite imagery. Active blind thrusts, normal and strike-slip faults, all leave their mark on surface topography as hills, scarps or valleys. Much of our understanding of planetary geology is derived from the analysis and interpretation of extraterrestrial landforms and landform interrelationships (e.g., PHILLIPS *et al.*, 2001).

The topography on passive margins of continental plates is shaped largely through the processes of denudation. Weathering and erosion carve topographic features through ancient structural and sedimentation patterns. Active tectonic processes in such environments may be limited to isostatic rebound in response to continued weathering and erosion. In an active tectonic environment such as Japan, tectonic processes including subsidence and uplift play a dominant role in shaping surface topography.

The influence of tectonics on the shape of Japan's surface topography is evaluated in the following study using maps of Quaternary vertical displacement and active fault distribution, along with recent measures of horizontal crustal strain covering 10- and 110-year time periods.

The methods employed in this paper allow us to compare the complex patterns formed by Japan's topographic surface and active fault system, to the scalar attributes of elevation and Quaternary vertical displacement (3 million year time frame), and horizontal crustal strain (110- and 10-year time periods).

2. Data Sets Used in the Study

A. Elevation

Elevation data throughout Honshu, Japan were extracted from the Geographical Survey Institute of Japan's 250 m digital mesh CD-ROM (GEOGRAPHICAL SURVEY INSTITUTE, 1997a). The sample interval in the east-west direction is approximately 230 meters throughout Honshu. In the north-south direction the sample interval varies from about 290 m near 34 degrees north latitude to 265 m near 41 degrees north latitude.

B. Active Faults

The geometrical properties of Japan's active fault complex provide another measure of recent tectonic activity in Japan. Movements along faults designated as active faults in Japan extend from the present day through the Quaternary, and thus impart, accommodated both short-term (recent 10- and 110-year periods) and long-term (Quaternary) responses to tectonic stress. In the comparisons undertaken in this study, fractal analysis is used to quantify the geometrical properties of the active fault complex. Prior studies have been undertaken of the fractal properties of Japan's active fault network (Fig. 2). Active fault traces were digitized from the 1:200,000 active fault maps prepared by the RESEARCH GROUP FOR ACTIVE FAULTS OF JAPAN (1991). HIRATA (1989) undertook a comprehensive evaluation of the fractal characteristics of Japan's active fault complex. HIRATA (1989) employed the box-counting method to estimate fractal dimensions, but unlike the approach used in the

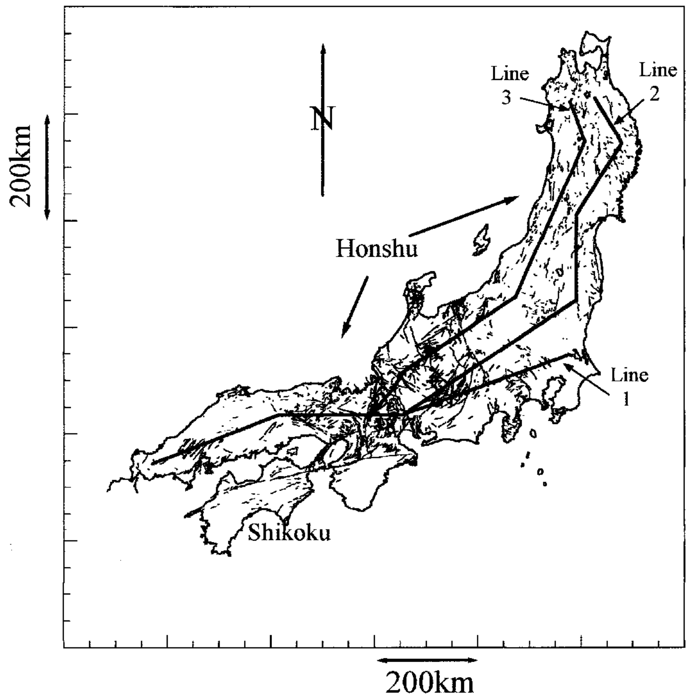

Figure 2
Active faults in Japan digitized from the 1:200,000 active fault maps produced by the RESEARCH GROUP FOR ACTIVE FAULTS OF JAPAN (1991).

present study, his box coverings were limited to base 2 variations in box size. HIRATA (1989) differentiated faults into two types based on the presence of a branching geometry (Type I) and a fragmented geometry with no main fault (Type II). For both types, highest fractal dimensions were encountered in the central part of Japan. Analysis conducted by WILSON (2001) and ONCEL *et al.* (2001) reveal scale-variant behavior throughout Japan's active fault network. Their analysis also employed the box-counting method. Use of this method involves covering the surface fault trace pattern with boxes of varying size and counting the number of boxes (N) of size r required to cover the pattern. The relationship of log (N) to log (r) is linear if the pattern is fractal. However, in many instances this linearity is not maintained over all scales; slope transitions occur. Abrupt slope transitions are encountered throughout the fault network in Japan; the slope transitions occur, on average, around 8 kilometers (see WILSON, 2001). SCHOLZ (1995) notes that abrupt and gradual transitions are often observed in natural objects. SCHOLZ (1995) notes their presence, for example, in power spectra of sea-floor topography and in the wavelengths of fault traces comprising the San Andreas fault system. WILSON (2001) also noted that transitions are commonplace in natural fracture patterns. Model studies conducted by WILSON (2001) attribute scale transitions to average spacing and fragment size in the more penetrative fault patterns or to average spacing and gap length in the more fragmented fault patterns. Transitions observed in Japan's active fault network are generally abrupt in nature. Features in the fault network examined over the 8–17.5 km range have higher fractal dimension than do features in the 2–8 km range. On average the fractal dimension over the 2–8 km range is 1.06 and that over the 8–17.5 km range, 1.39. Standard deviations on the estimates of fractal dimension were on average 0.09 over the 8–17.5 km range and 0.03 over the 2–8 km range, making these range-limited estimates of fractal dimension significantly different at the 95% confidence level.

Contours of active fault fractal dimension (D_{AF}) estimated over the 2–8 km range along lines 1 through 3 are shown in Figure 3; D_{AF} is highest in central Japan, and is consistent with HIRATA'S (1989) earlier analysis. In general, areas of higher D_{AF} correspond to more intensely faulted regions, whereas regions of smaller D_{AF} correspond to less intensely faulted areas.

Fractal representation of topography and active fault patterns allows us to make direct comparison of these complex variables to Quaternary vertical displacements and crustal strain.

C. Quaternary Vertical Displacement

Quaternary vertical displacements (QVD) in Japan (Fig. 4) were taken from the Research Group for Quaternary Tectonic Map (RGQTM, 1973). Mapped displacements were estimated from elevations of late Pliocene and early Pleistocene erosion surfaces and from elevations of the contact between marine Pliocene and Pleistocene

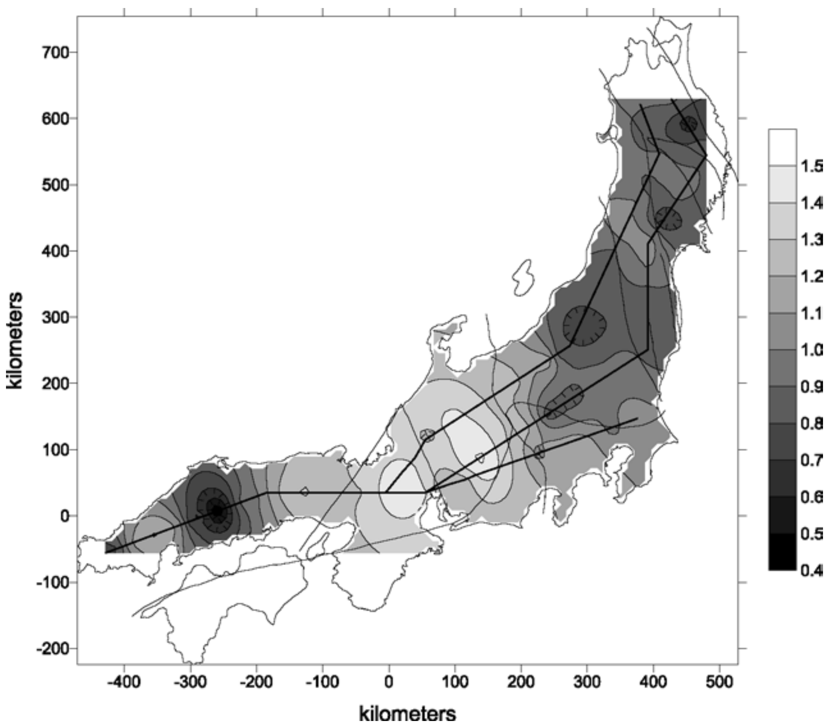

Figure 3
Contours of the range limited (2-to-8 km) fractal dimension of active faults (D_T) computed along the three analysis lines.

formations (RGQTM, 1973). The Research Group for Quaternary Tectonic Map (1973) attributes present-day elevation variation throughout Japan primarily to Quaternary tectonic movements.

Mapping of erosion surface elevation was possible only in uplifted regions. Some error in these estimates is expected since the erosion surfaces are assumed to have formed at sea-level (RGQTM, 1973). Additional error is related to the absence of late Pliocene and early Pleistocene erosion surfaces in some areas. In these areas uplift could often be inferred from other erosion features. For example, erosion of upper Miocene surfaces was assumed in some places to have taken place during the late Pliocene or early Pleistocene (RGQTM, 1973).

These geomorphological estimates were combined with geological estimates obtained by mapping elevations of boundaries between marine Pliocene and Pleistocene formations. The assumption that these horizons formed at sea level is a potential source of error. In addition, these formations, where uplifted, have generally experienced some erosion. In practice, the highest points of the upper Pliocene or lower Pleistocene were used to estimate vertical displacement in uplifted areas (RGQTM, 1973). Deep drilling data were used to locate depths of the

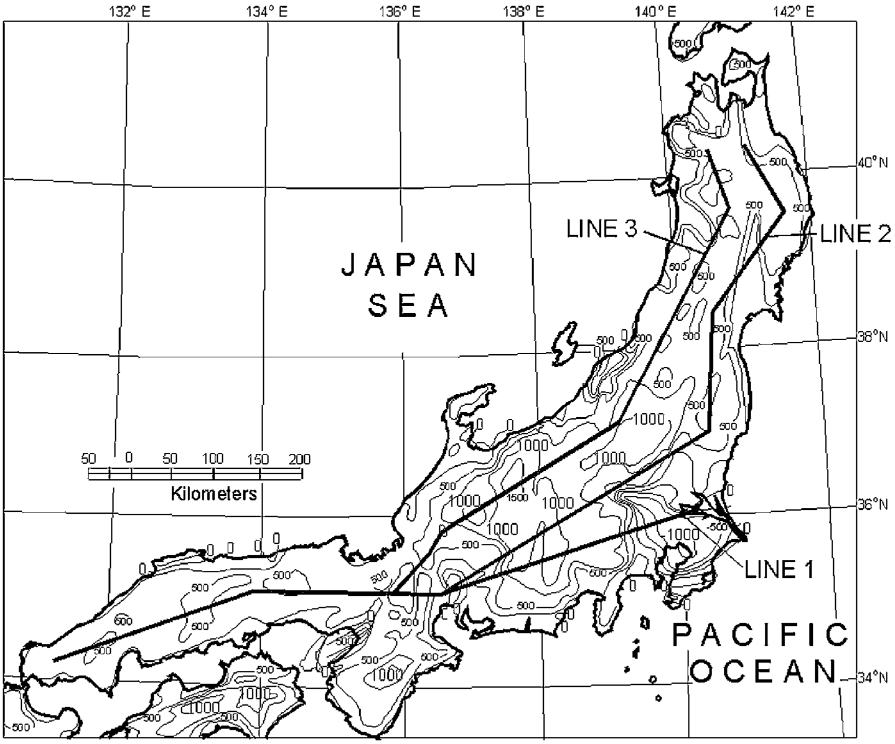

Figure 4
Contours Quaternary vertical displacement in meters are shown primarily for Honshu, the main island of Japan (after Research Group for the Quaternary Tectonic Map, 1973).

Plio-Pleistocene boundary in subsiding areas beneath alluvial and coastal plains, and interior basins. Relatively few data points are available and these were supplemented by assuming uniform subsidence rates to extrapolate depth to the base of the Pleistocene from the known depths of younger formations. Depths estimated from erosion-surface elevation tended to be about 200–300 m greater than those estimated from the Plio-Pleistocene boundaries observed in marine sediments (RGQTM, 1973). Adjustments of these differences were made on an area by area basis, and preference was given to data evaluated as being the more reliable in any given area (RGQTM, 1973).

D. Horizontal Crustal Strain

Short-term area and maximum shear strain data were taken from the Geographical Survey Institute's web site at http://cais.gsi.go.jp/HIZUMI/hizumi7.html. This site contains data used to construct the Horizontal Crustal Strain map of Japan (GEOGRAPHICAL SURVEY INSTITUTE, 1996, 1997b). The strain maps were compiled using measurements of about 2,400 stations spread throughout Japan. The data used in this study consist of 981 stations selected from the Geographical Survey Institute database over Honshu. Strain measurement data are available for recent 110- and 10-year time intervals. The 10-year database contains recent strain measurements made between 1985 and 1994. These strains were derived from first-order trilateration using an electronic distance-measuring device (Ishikawa *et al.*, 1998; Yagi, personal communication, 1999). The 110-year data cover the time period from 1883 to 1994 and were derived from first-order triangulation measurements. Calculated horizontal area strain and maximum shear strain were gridded and contoured. Contoured area strain data for 10- and 110-year time periods are shown in Figures 5A and 5B, respectively. Strain data were extracted from the contour maps along lines 1 through 3 for comparison to the fractal properties of the active fault complex and to other variables in the study examined along these lines.

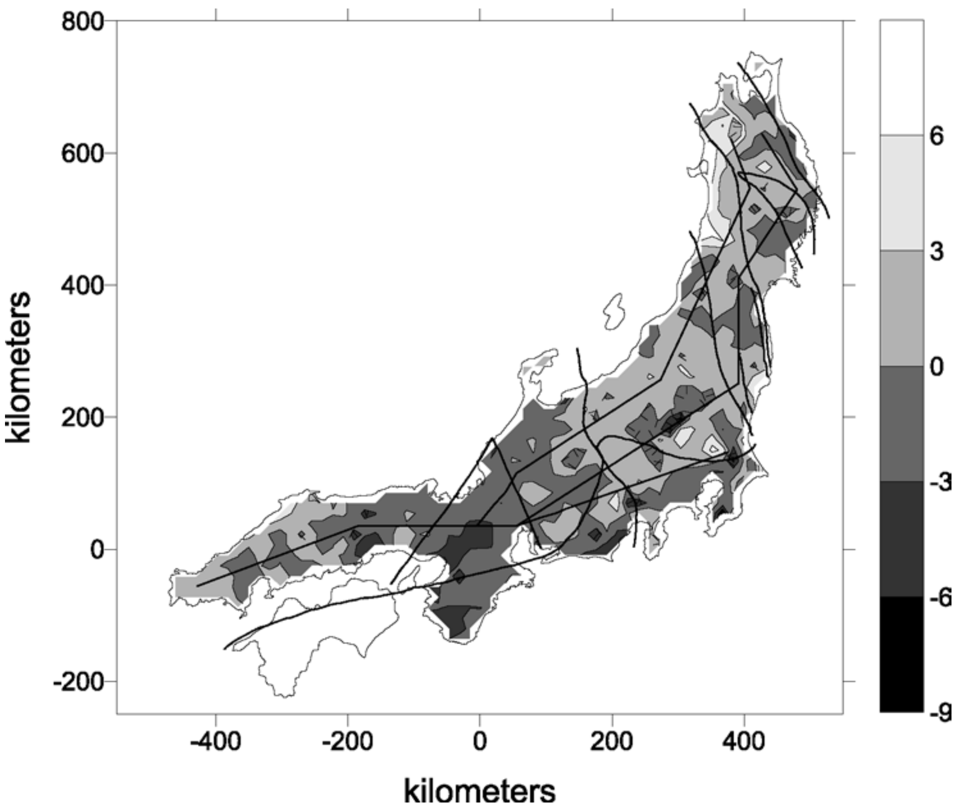

Figure 5A
Horizontal area strain ($\times 10^{-6}$) estimated over a 10-year time period extending from 1985 through 1994. The zero contour line is labeled for reference.

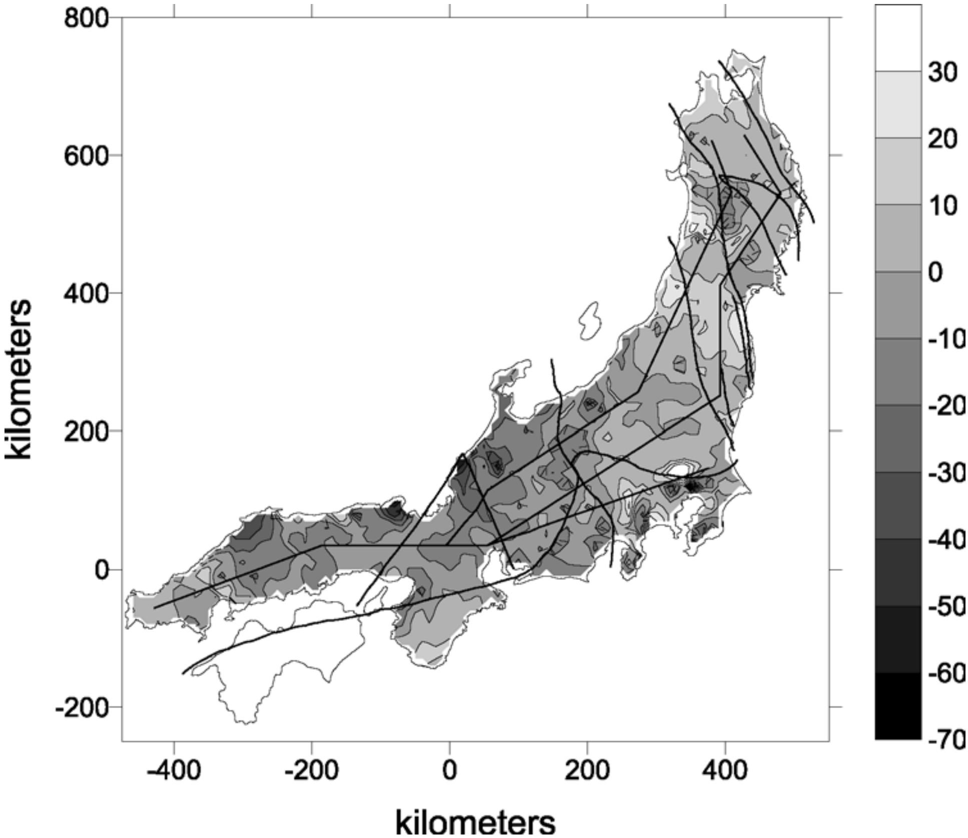

Figure 5B
Horizontal area strain (× 10^{-6}) estimated over a 110-year time period that extended from 1883 to 1994. The zero contour line is labeled for reference.

3. *Methods of Analysis*

A. Estimating the Fractal Dimension of Elevation Variation

Fractal analysis of topography throughout Japan conducted in the present study was undertaken along 70 km long north-south and east-west profiles extracted throughout Honshu on a roughly 10-km grid within the 250 m digital elevation data set for Japan (GEOGRAPHICAL SURVEY INSTITUTE, 1997a). The fractal dimension of elevation provides a measure of surface roughness. A high fractal dimension generally corresponds to greater surface roughness than does a low fractal dimension. The fractal dimension of a profile can be estimated using several different methods. In addition these estimation procedures can be classified as either self-affine or self-similar. The roughness-length estimate (MALINVERNO, 1990), for example, provides a self-affine measure of the fractal dimension of topography. A self-affine estimate is usually employed to compute the fractal properties of functions in which the units along the x-axis differ from those along the y axis describing the function: e.g., the variation of magnetic field intensity as a function of time (TURCOTTE, 1992). TURCOTTE (1992) suggests that surface topography is self-affine. FOX (1989), MALINVERNO (1990) and MARESCHAL (1989) consider sea-floor topography to be self-affine.

B. Self-Affine Estimates of Fractal Dimension

MATSUSHITA and OUCHI (1989) note that self-affinity can be defined based on the presence of directional differences in the log-log relationship of standard deviation in elevation versus curve length or window size. They suggest that the occurrence of different slopes in the log-log relationship obtained along the horizontal (the sample points) and vertical (elevation) directions would imply that data are self-affine. They find differences in the relationship between standard deviation and curve length in the horizontal and vertical directions for topographic relief near Mt. Yamizo and Mt. Shirouma and conclude that topography is self-affine. However, we would note that the slope of the log-log relationship obtained for the horizontal sample locations will always tend to 1.0 since the data along the horizontal direction consist of a series of points separated by a constant sample interval. This will be the case along the horizontal for all profile data and other single valued series of points separated by a constant sample interval.

WILSON (2000) notes that self-similar and self-affine measures of the fractal properties of curves provide different information. In the case of topographic data the units along the horizontal and vertical axes are the same and it is possible to use either self-affine or self-similar measures of the fractal properties of topographic profiles depending upon the objectives of the study. WILSON (2000), for example, undertook an analysis of structural profiles using roughness-length (self-affine) and compass (self-similar) measures of fractal properties. In that study, the self-similar compass dimension could be related directly to profile length and to shortening whereas the roughness-length dimension was not easily related to specific physical properties of the profiles.

In the present study, both self-affine and self-similar fractal dimensions of topography were computed. The roughness-length method (MALINVERNO, 1990) was used to make self-affine estimates of fractal dimension. The roughness-length measure is based on the following relationship (TURCOTTE, 1989, 1992),

$$\sigma = \tau^{H} \quad , \tag{1}$$

between the standard deviation of elevation (σ) and length of window (τ) over which σ is computed. H is referred to as the Hurst exponent (FEDER, 1988) and is related to D through the relationship

$$D = 2 - H \quad (2)$$

(e.g., TURCOTTE, 1989). σ is computed from the average standard deviation of data in each of the τ-length subdivisions of the profile. Initially, τ equals the length of the profile and is subsequently diminished in size by a factor of 2 at each step. As the window length (τ) decreases, σ is normally computed from the average standard deviations within 1, then 2, 4, 8, etc., subdivisions of the profile. Log-log plots of σ versus τ are linear with slope H, as implied by Equation (1) if the data have a fractal distribution. In this study, we use a modified approach to the roughness-length computations (WILSON, 2001) that incorporates smaller logarithmic decreases in window size. The slope of the roughness-length (σ *vs.* τ) plots was in general not constant (Fig. 6). Minor variations of slope were observed throughout Japan. Slope breaks were often encountered in the τ = 6 to 10-km range, so separate slope computations were made over the 2 to 8-km and 8 to 18 kilometer range throughout Japan. Contour maps of the self-affine (roughness-length) measure of fractal dimension (Figs. 7A and B) over the 2-to-8 and 8-to-18 km ranges, respectively, exhibit fairly random patterns of variation and do not differentiate between low and high-relief areas, which are important to the assessment of tectonic influences. The self-affine measures of the fractal properties of topography in general did not reveal significant correlation to the variables being investigated in this study.

C. Compass Estimates of the Fractal Dimension

As noted above, the compass dimension can be directly related to profile length and provides an estimate of length that incorporates the fractal properties of the profile. Thus the compass dimension provides physical information about elevation profiles that might have direct relationship to other physical properties such as vertical uplift and crustal strain. The compass dimension of elevation variation provides a

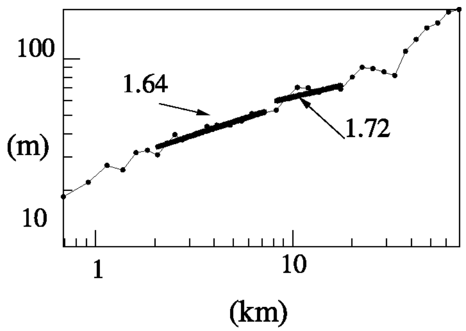

Figure 6
Roughness-length plot for elevations in the Hiroshima area of southwestern Japan. Self-affine estimates of fractal dimension were made over the 2-to-8 km and 8-to-18 km range as shown above. τ is the window length, and σ is the standard deviation of elevations in the τ-length window. Regression lines computed for the 2-to-8 km and 8-to-18 km ranges are shown.

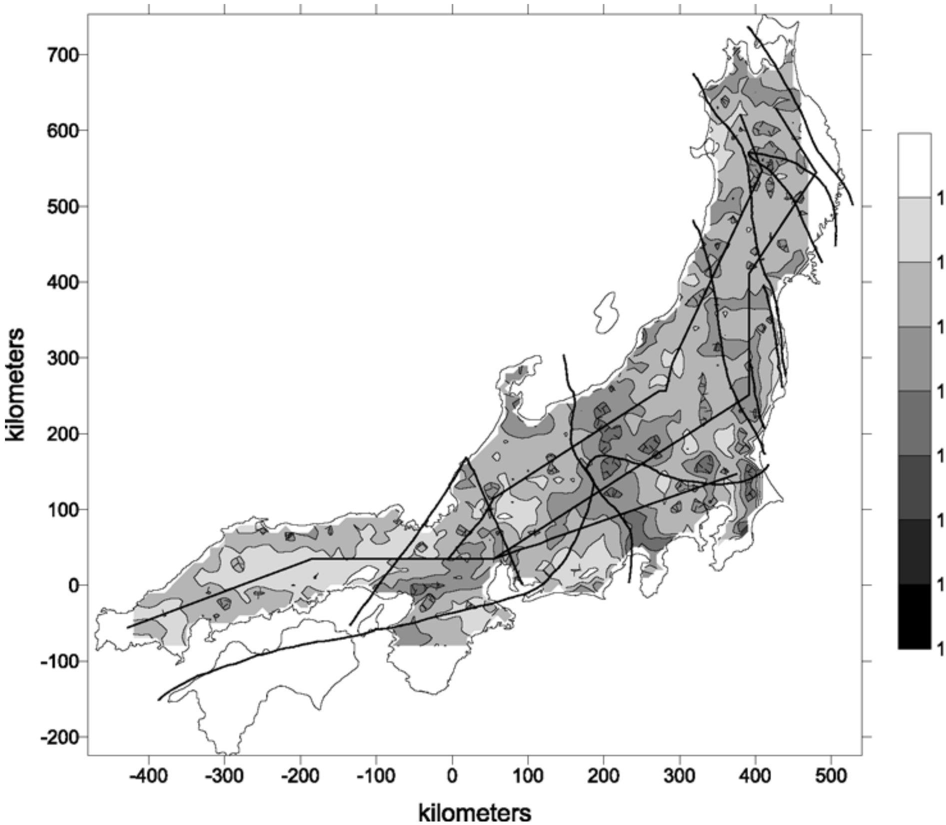

Figure 7A
Contours of the roughness-length dimension of elevation computed over the 2-to-8 km range.

measure of surface roughness that can be directly related to other physical properties, such as, elevation variation, Quaternary vertical displacement (QVD) (Fig. 4), crustal strain, and also to the fractal properties of the active fault complex (D_{AF}) (Fig. 3).

The compass method of computing the fractal dimension (MANDELBROT, 1967) is made by walking along a profile with steps of different length. If N steps of length r are required to walk along a curve, then the curve has length $L = Nr$ at scale r. If the relationship between the number of steps (N) of length r varies as Cr^{-D}, then the curve is said to be fractal and to have fractal dimension D. The length of the curve L is Nr, but L in this case increases as Cr^{1-D}. The path along the topographic surface is a fractal path along which path length increases non-linearly with decreases in step-size.

Compass-walks were taken along topographic profiles extracted from the 250 m digital mesh (GEOGRAPHICAL SURVEY INSTITUTE, 1997a) in north-south and east-west directions. Sample interval in the east-west direction is approximately 230 meters throughout Honshu. In the north-south direction the sample interval varies from about 290 m near 34 degrees north latitude to 265 m near 41 degrees

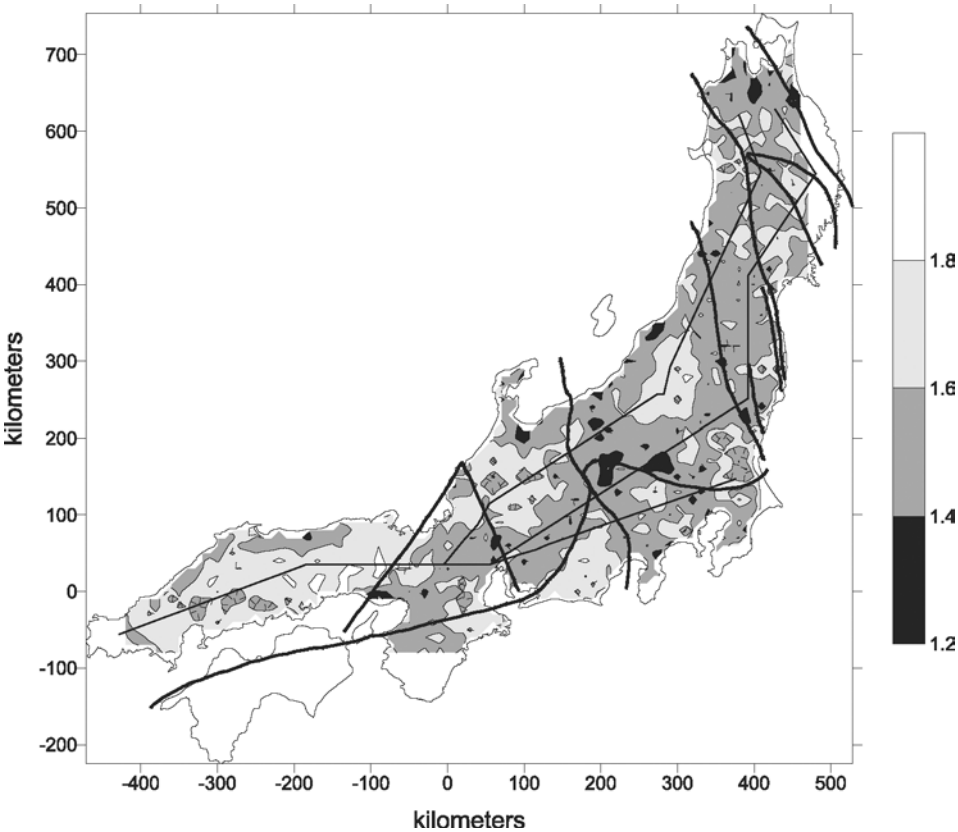

Figure 7B
Contours of the roughness-length dimension of elevation computed over the 8-to-18 km range.

north latitude. NS and EW oriented profiles were extracted at approximately 10-km intervals and the fractal dimension was computed roughly every 10 km along each profile. The NS and EW estimates were averaged. Results were interpolated onto a 10-km grid to construct the contour plot shown in Figure 8. Points were extracted from the grid at 20-km intervals along lines 1 through 3 used in the analysis of the active fault network mentioned above. The extracted points were used for intercomparison of data along lines 1 through 3.

In the relationship $N = Cr^{-D}$, the graph of log N vs. log r forms a straight line with slope D. Analysis of these log N vs. log r plots in several areas throughout Japan reveals that the relationship is slightly nonlinear (e.g., Fig. 9). D varies with scale, which implies that elevation variation is not purely fractal. D often increases with smaller step size (r). Although the differences in slope shown in Figure 9 are very small, the slope for scales (r) greater than 18 km is significantly less than that observed over the 2-to-8 and 8-to-18 km scale ranges at the 95% confidence level.

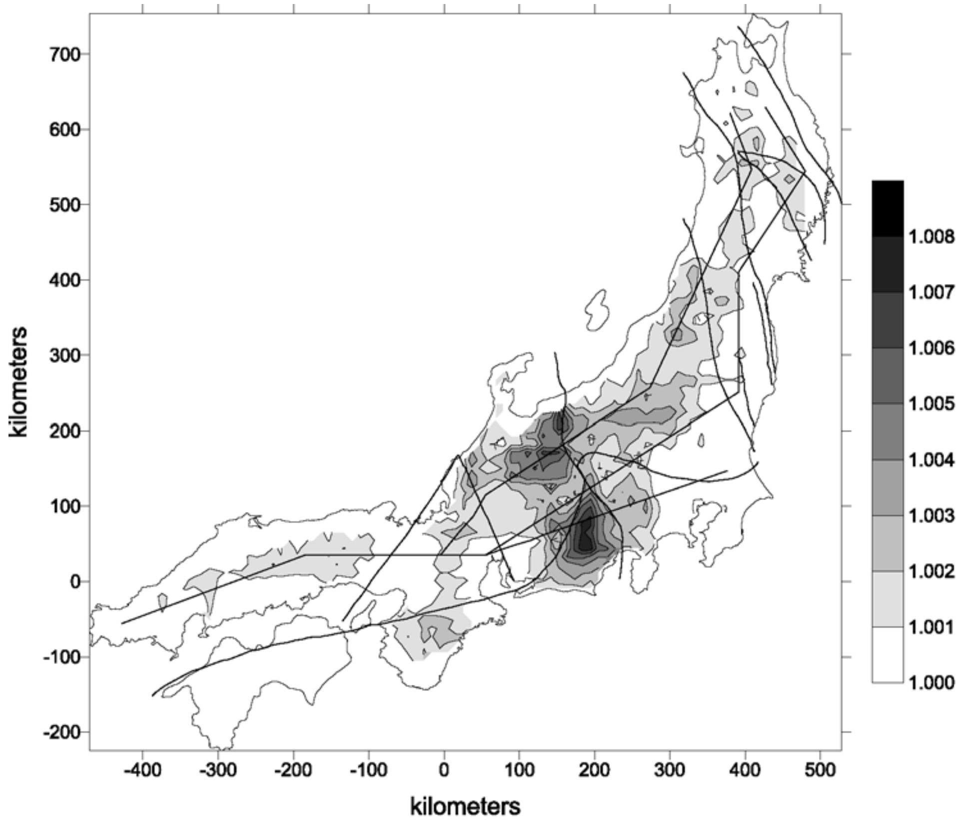

Figure 8
Compass-walk estimates of the range-limited fractal dimension of topographic relief (D_T) computed over the 2–8 km range along EW and NS profiles. The contours are derived from an average of the EW and NS values computed at each point along lines 1 through 3.

Likewise the slope for *r* less than 2 km is statistically higher than that observed for larger *r*. As in the active fault analysis, *D* was estimated over roughly the 8-to-18 km range and 2-to-8 km range. Estimates of *D* over the 8-to-18 km range (not shown) vary between 1 and 1.004; over the 2-to-8 km range, *D* varies between 1 and 1.011. The 2-to-8 km range estimates of fractal dimension (Fig. 8) provide a more detailed view of the variability in the fractal properties of topography throughout Japan. The 2-to-8 km data are used for comparison with other variables.

4. *Tectonic Framework of Japan*

The spatial distribution of structural elements within Japan provides a tectonic framework within which strain and uplift can be referenced. The islands of Japan

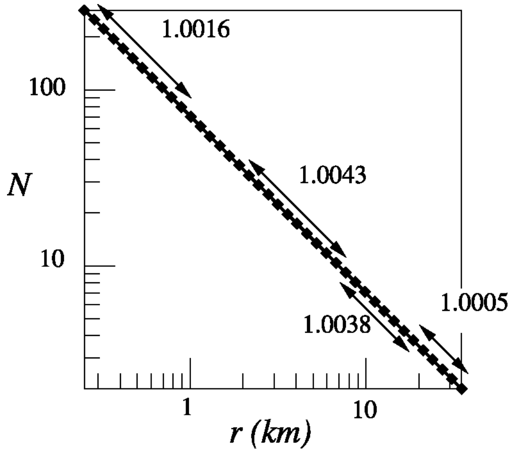

Figure 9
Results of the compass-walk along a topographic profile reveal subtle changes of slope over step-sizes (r) ranging from 35 km to approximately 250 m.

are comprised of ancient crustal fragments, numerous accretionary complexes and suture zones (Fig. 10) whose formation spans the Phanerozoic and Proterozoic eons. Paleozoic-to-recent accretionary complexes are built above a backbone of Proterozoic metamorphic complexes that once comprised the supercontinent of Rodinia (ISOZAKI, 1996; WAKITA, 1997). Approximately 450–500 Ma passive margin conditions gave way to subduction and since that time Japan has remained an active continental margin (KANO and WAKITA, 1992; ISOZAKI, 1996; WAKITA, 1997). More recently (early Miocene), Japan separated from the Eurasian continental margin through the process of backarc spreading (TAMAKI, 1988; JOLIVET and TAMAKI, 1994). During the opening of the Japan Sea, northeast Japan was partly decoupled from southwest Japan across the Tanakura Tectonic Line (TTL) (Fig. 1). Disorganization of earlier accretionary complexes is much more significant in northeast Japan than in southwest Japan since northeast Japan is cut by several left-lateral strike-slip faults (ISOZAKI, 1996). Offsets across these faults, which include the TTL and Hatagawa Tectonic Line (HTL) (Fig. 1), accommodated counterclockwise motion of northeast Japan away from the Eurasian plate.

Transpressional plate convergence in the forearc region of southwestern Japan has produced strike slip offsets through the system of complexes in the outer arc region along the Median Tectonic Line (MTL, Figs. 1 and 10). The MTL lies along the northern boundary of the Nankai forearc sliver (northwest of Nankai Trench), which is driven westward by oblique subduction of the Philippine Sea Plate beneath the Eurasian Plate in southwest Japan (Fig. 10) (TSUKUDA, 1992). Movement along the MTL is predominantly right-lateral strike-slip but has experienced significant reverse motion, at least during the Plio-Pleistocene (OKADA, 1980). The reverse component is southeast vergent. The 1995 Hyogo-ken Nanbu

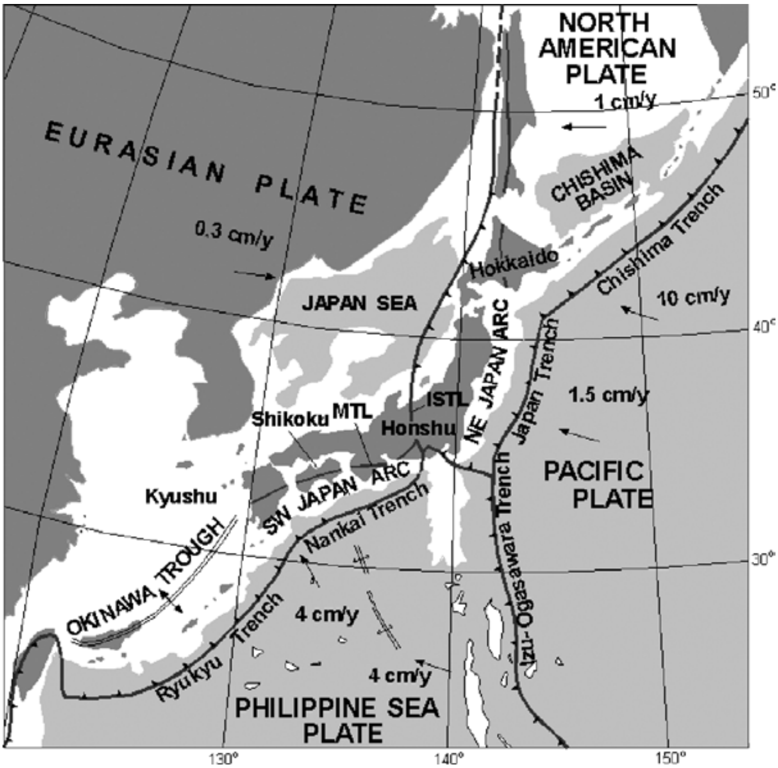

Figure 10
Regional tectonic setting of Japan (after KANO and WAKITA, 1992).

(M 7.2) earthquake occurred along a northeast trending strike-slip fault that branches off the MTL and extends through the island of Awaji to Kobe (Fig. 1). Mapped displacements reveal as much as 1.7 meters of right-lateral movement along with a maximum of 1.3 meters of vertical displacement. Active fault zones extending inland to the northeast of Kobe and the area north of the MTL to the Japan Sea form the Kinki Triangle (Figs. 1 and 10). The Kinki Triangle is defined by active strike slip faults along its northeast and northwest sides (TODA *et al.*, 1998). North-south trending reverse faults are dominant within the triangle (TODA *et al.*, 1998). The Kinki Triangle in addition to the MTL are believed to, in part, accommodate shortening of the Eurasian plate against the North American plate across the Itoigawa-Shizuoka Tectonic Line (ISTL) (Figs. 1 and 10).

The ISTL is believed to be an incipient subduction zone (NAKAMURA, 1983; KOBAYASHI, 1983) across which northeastern Japan is subducting beneath southwestern Japan. Recent excavation along the ISTL reveals the extent and possible recurrence interval of large earthquakes occurring on individual segments of the ISTL during the last 5,000 to 7,000 years (OKUMURA et al., 1994; OKUMURA, 2001). A low velocity zone observed in a seismic refraction profile across the ISTL (IKAMI et al., 1986) coincides with a southwest dipping low density zone inferred from gravity models along the profile (WILSON and KATO, 1992 and 1995). A zone of seismicity in the backarc area of northern Japan punctuated by recent large earthquakes (*M* 7.7 and *M* 7.3 in 1983 and 1993, respectively), is suggested to be associated with the northern extension of this subduction zone (Fig. 10) along the western boundary of the North American Plate (e.g., SHIMOKAWA, 1997). Analysis of 1997–1999 GPS derived displacement rate vectors presented by SAGIYA *et al.* (2000) reveals abrupt changes in plate velocity across a zone which extends north to south along the Japan Sea side of Honshu and cuts through southwestern Honshu toward Shikoku along the western margin of the Kinki Triangle. They suggest this zone may represent an incipient plate boundary. This zone is not evident in the area strain data (Fig. 5). However, in both the 10- and 110-year area strain maps (Fig. 5) the ISTL roughly separates a region of predominantly negative area strain in southwestern Japan from a region of predominantly positive area strains in northern Japan.

The slow convergence of the Eurasian Plate (0.3 cm/yr) toward the North American Plate across the ISTL is met on its southern end by collision with the Philippine Sea Plate (Fig. 10). The meeting point of these three plates forms a TTT triple junction just north of Mt. Fuji. The Philippine Sea Plate carries the Izu-Bonin arc northward in this area. This arc-arc collision produces the *V*-shaped indentation known as the Kanto Syntaxis west of Tokyo (KANO *et al.*, 1990; TAKAHASHI and SAITO, 1997) (Figs. 1 and 10). Paleomagnetic studies of Late Miocene diorite bodies in the Kanto Mountains suggest that the syntaxis formed in the late Miocene or earlier (TAKAHASHI and NOMURA, 1989; TAKAHASHI and SAITO, 1997).

The varied tectonic features that are mentioned above have all left their imprint, to varying degree, on the surface topography of Japan. Most noticeable are expressions of the MTL, ISTL and Kanto Syntaxis (Fig. 1). The high relief regions of central Japan, as a whole, coincide with areas of high Quaternary uplift (Fig. 4). The eastern boundary of the high relief/high uplift region of central Japan coincides approximately with the Tanakura Tectonic Line (TTL). To the west, this high relief/uplift region is bounded by the eastern margin of the Kinki Triangle. The active fault pattern on the other hand reveals an abrupt decrease in fault density east of the ISTL (Fig. 2). The Kinki Triangle to the west is also intensely faulted. However, Quaternary uplift is generally less than 500 m in the Triangle, suggesting that displacements along the north-south trending reverse faults in the interior of the Kinki Triangle have not been extensive.

Table 1

Average correlation coefficients between variables along lines 1 through 3. QVD—Quaternary vertical displacement; T—elevation; D_T—fractal dimension of elevation variation; D_{AF}—fractal dimension of active fault network; AS10—10-year area strain; AS110—110-year area strain; MS10—10-year maximum shear strain; MS110—110-year maximum shear strain

	QVD	T	D_T	D_{AF}	AS10	AS110	MS10	MS110
QVD	1	0.75	0.75	0.08	0.19	−0.01	−0.06	−0.21
T		1	0.69	0.13	0.20	0.08	−0.13	−0.18
D_T			1	0.33	0.17	0.0	−0.09	−0.02
D_{AF}				1	−0.43	−0.26	0.17	0.24
AS10					1	0.48	−0.05	0.03
AS110						1	0.14	−0.08
MS10							1	0.01
MS110								1

5. *Results*

A. Regional Correlation between Data Sets

The average correlation coefficients ($\langle r \rangle$) obtained from comparisons of the variables discussed above for all three lines combined are listed in the correlation table above (Table 1). The highest correlations ($\langle r \rangle = 0.75$) occur between T (elevation) and D_T (the range-limited fractal dimension of elevation) with Quaternary vertical displacement (QVD) (Table 1). The correlation of D_T to T is slightly less ($\langle r \rangle = 0.69$). Correlations of the 10- year and 110-year strain measures with topography, Quaternary vertical displacement and active faulting are generally low. A relatively large negative correlation between 10-year area strain and active fault fractal dimension ($\langle r \rangle = -0.43$) is observed. The correlations between the 10- and 110-year strains are surprisingly low and highlight the greatly variable nature of strain over these short time intervals.

Comparison of elevation variation and Quaternary vertical displacement (Fig. 11) along Line 3 (see locations in Figs. 2 and 4) reveals considerable similarity. On average, QVD along Line 3 through southwest Japan is relatively low, around 500 m (Fig. 11A). Elevation in southwest Japan is also relatively low and averages around 250 m on Line 3 (Fig. 11B). Elevation and QVD rise east of the Kinki Wedge (around 500 km along the line) toward the ISTL (at approximately 650 km). Both QVD and elevation decrease considerably (600 m and 1500 m, respectively) across the ISTL. To the north of the ISTL through northern Japan along Line 3 there is a general south-to-north decrease in both QVD and relief. The high relief and high QVD areas of central Japan also coincide with a region of thickened crust produced by the convergence of plates that takes place in central Japan (e.g., SUGIMURA and UYEDA, 1973).

Variations in D_T (Fig. 8) have direct relationship to visually recognizable topographic and structural features. The most conspicuous features in the contour

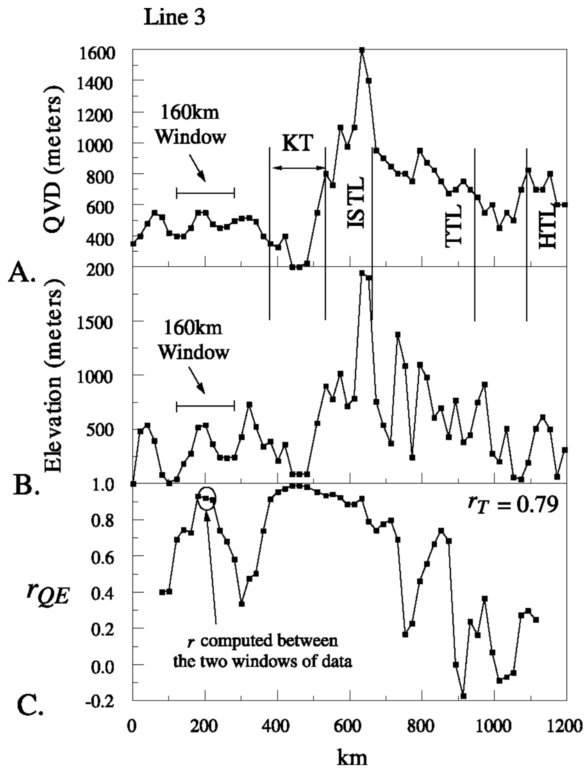

Figure 11
A) Quaternary vertical displacement (QVD) along Line 3; B) elevation (T) along Line 3; C) local correlation coefficients (r_{QE}) between QVD and T along Line 3. r_T is the correlation coefficient computed for the entire line. KT = Kinki Triangle, ISTL = Itoigawa-Shizuoka Tectonic Line, TTL = Tanakura Tectonic Line, and HTL = Hatagawa Tectonic Line.

map are the areas of high D_T located in central Honshu between the Itoigawa-Shizuoka Tectonic Line (ISTL) and Kinki Triangle. The high D_T region near the northern end of the ISTL coincides with the Hida Mountains that bound the ISTL to the west, while the high near the southern end coincides with the rugged mountainous area of Kofu which is bounded by the Median Tectonic Line (MTL) on the west and ISTL on the east. The Hida and Kofu areas are anomalously rugged when compared to areas across the ISTL in northeast Japan that are only a few hundred meters lower in elevation.

B. Local Variability in the Correlation between Data Sets

Variations in spatial correlation between variables along each line is examined in local detail by computing correlation coefficients for smaller windows or subsets of the data along each analysis line. Correlation coefficients (r) were computed between

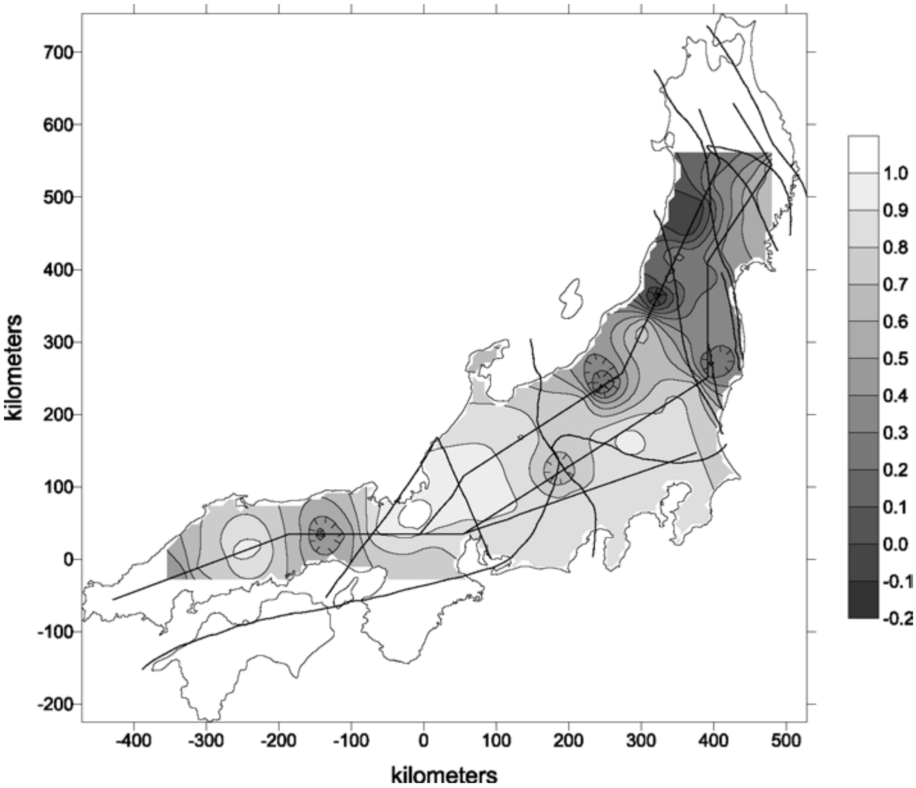

Figure 12
Contours of the local correlation between Quaternary vertical displacement (QVD) and elevation (*T*) computed along lines 1 through 3.

160 km subdivisions of the data every 20 km along Lines 1 through 3. Thus, each data point in the correlation plot (e.g., Fig. 11C) corresponds to the correlation coefficient computed between a 160 km long window of the elevation and QVD data centered at that point on the profile (see marked windows in Fig. 11). Spatial correlation between QVD and elevation along line 3 (Fig. 11C) defines a region of high positive correlation that extends through the Kinki Triangle (located about 400–500 km along the line) and across the ISTL (650 km). The correlation drops continuously north of the ISTL. Contours of the local correlation computed from all three lines (Fig. 12) reveal consistently high correlation between QVD and elevation through the Kinki Triangle northward across the ISTL and eastward across the Kanto plains to the Tanakura Tectonic Line (TTL). In the northern part of the region between the ISTL and TTL (the northern Fossa Magna (Fig. 1)) there is somewhat lower correlation than is found to the south beyond the MTL through the Kanto Plain area. Northeast of the TTL the correlation is generally low.

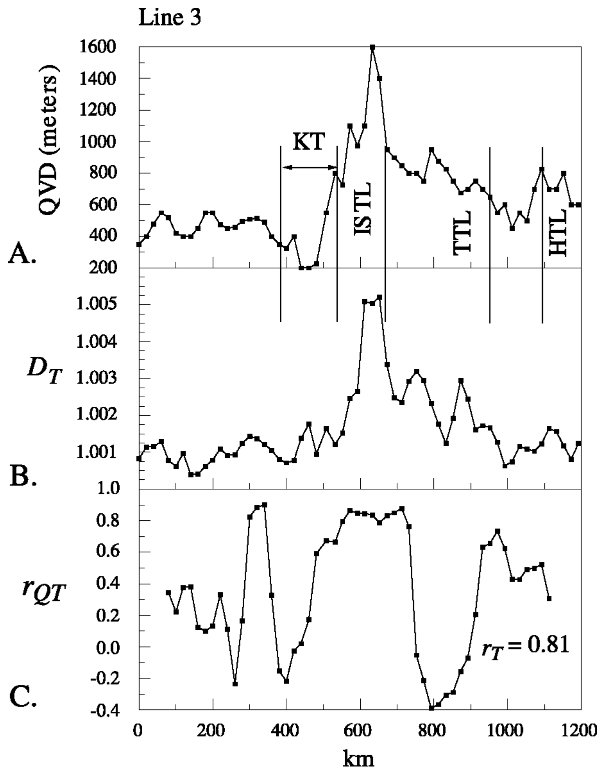

Figure 13
A) Quaternary vertical displacement (QVD) along Line 3; B) variations in the fractal dimension of topographic relief (D_T) along Line 3; C) local correlation coefficients (r_{QT}) between QVD and D_T along Line 3. r_T is the correlation coefficient computed for the entire line. KT = Kinki Triangle, ISTL = Itoigawa-Shizuoka Tectonic Line, TTL = Tanakura Tectonic Line, and HTL = Hatagawa Tectonic Line.

Comparison of the fractal dimension of elevation variation (D_T) to QVD along Line 3 (Fig. 13) reveals some similarity to that obtained between QVD and elevation (Fig. 11B). The fractal dimension (D_T) (Fig. 13B) is low in southwest Japan and increases across central Japan to a maximum in the Hida Mountains area (approximately 600–650 km along the line). D_T drops abruptly northward across the ISTL and continues to drop (with smaller gradient) through northeast Honshu. The local correlation between D_T and QVD along Line 3 (Fig. 13C) rises from a low along the western end of the Kinki Triangle to a high, which is maintained across central Honshu and the ISTL into the northern Fossa Magna region. Contours of the local correlation along all three lines (Fig. 14) reveal that the high observed on Line 3 continues across the southern part of the Fossa Magna through the Kanto Plain. A region of low correlation develops in the northern part of the northern Fossa Magna that extends across the TTL (Fig. 14). Overall, the general features of the two data sets (D_T and QVD) are

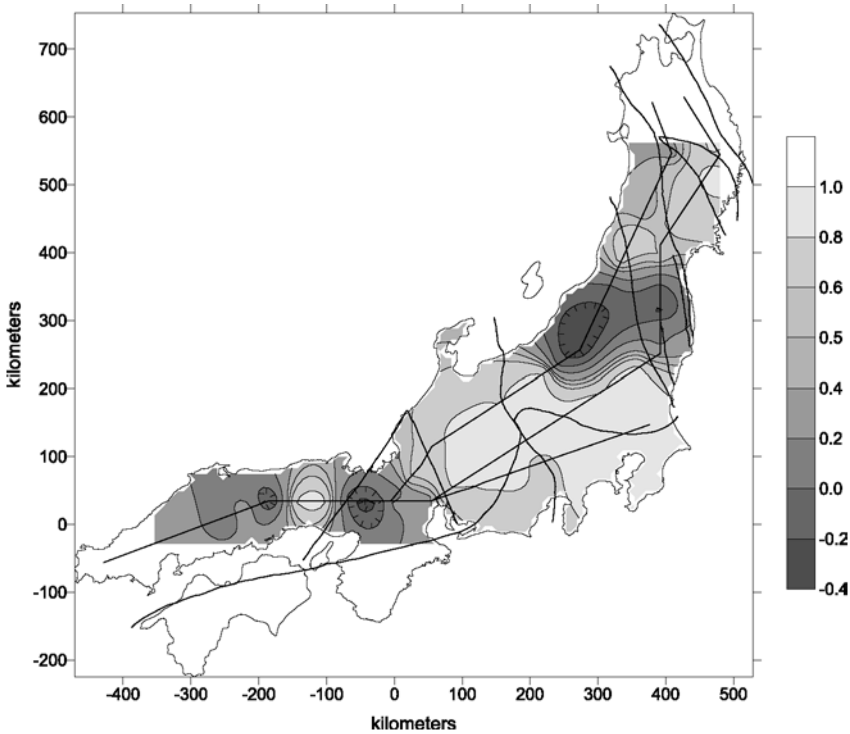

Figure 14
Contours of local correlation coefficients (r_{QT}) between Quaternary vertical displacement and fractal dimension of topographic relief (D_T) along lines 1 through 3.

quite similar ($r = 0.81$). Variations in the local correlation are associated with interrelationships at scales of 160 km and less. The local correlation is consistently high through central Japan and, not surprisingly, suggests that increased surface roughness measured by D_T is associated with high tectonic uplift. The tectonic significance of low and high correlation elsewhere along the length of Honshu is more questionable.

The correlation between elevation (T) and the range-limited fractal dimension (D_T) of elevation variation shown in Figure 15C forms a pattern similar to that observed between QVD and D_T (Fig. 13C). The local correlation between D_T and QVD rises eastward across the Kinki Triangle into central Japan and drops abruptly northeast of the ISTL into the northern Fossa Magna region. The high correlation region in central Japan is associated with similar change in the major features of D_T and elevation. In general however, the pattern of variability observed in the correlation contours is not clearly divided by individual structural boundaries.

The relationship between the range-limited fractal dimensions of the active fault patterns (D_{AF}) and elevation variation (D_T) reveals low correlation through the Kinki Triangle and central Japan Alps, with higher correlation occurring north

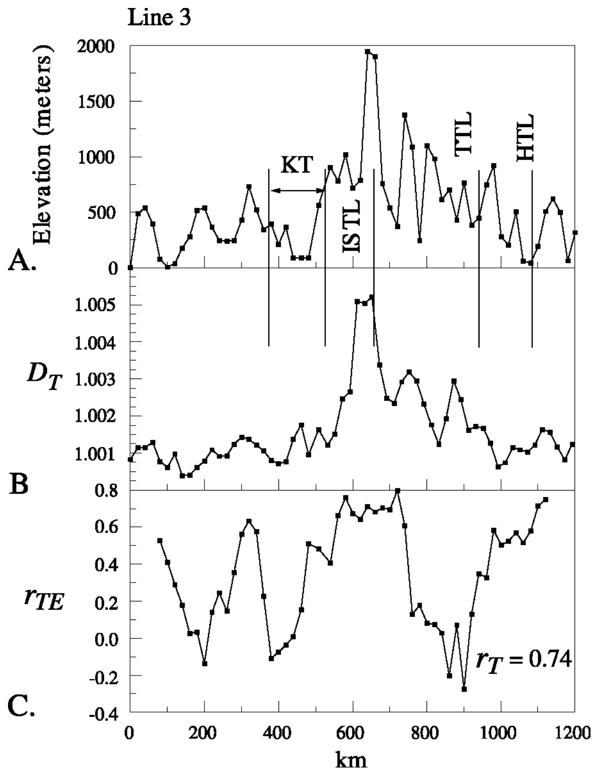

Figure 15
A) Profile of elevation variations (T) along Line 3; B) profile of the fractal dimension of topographic relief (D_T) along Line 3; C) local correlation coefficients (r_{TE}) between D_T and elevation along Line 3. r_T is the correlation coefficient computed for the entire line. KT = Kinki Triangle, ISTL = Itoigawa-Shizuoka Tectonic Line, TTL = Tanakura Tectonic Line, and HTL = Hatagawa Tectonic Line.

across the ISTL and west beyond the Kinki Triangle. The average correlation coefficient between D_{AF} and D_T computed from all three lines is 0.33. Areas of considerable complexity in the active fault network that are not correlated with QVD may have accommodated predominantly strike slip displacements. The Kinki Triangle is an area of considerable fault complexity where QVD and elevation are relatively low but highly correlated (see Fig. 11). The low correlation between D_{AF} and QVD suggests that active faulting during the Quaternary in the Kinki Triangle area was dominated by strike-slip displacements.

Correlation between 10-year horizontal area strain and active fault fractal dimension (D_{AF}) has, overall (Table 1), negative correlation ($r_T = -0.43$). Comparison of the variations between 10-year area strain and D_{AF} shown along Line 3 (Fig. 16) reveals a regional trend of decreasing or negative area strains in the highly faulted (high D_{AF}) regions of southwestern and central Honshu (Fig. 5A). This general trend also appears on lines 1 and 2 (not shown). The local

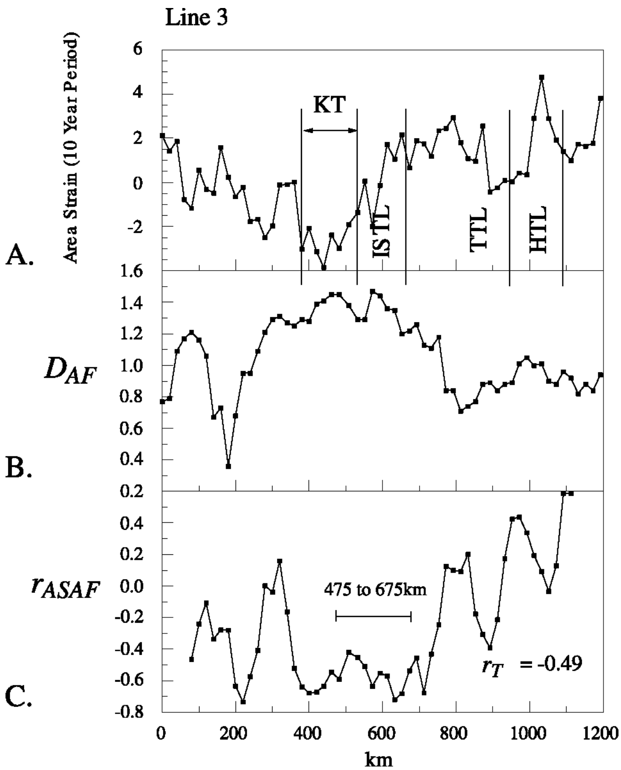

Figure 16
A) The 10-year area strain variations ($\times 10^{-6}$) are plotted along Line 3; B) variations of the fractal dimension of active faults (D_{AF}) along Line 3; C) variations in local correlation coefficients (r_{ASAF}) between D_{AF} and 10-year area strain. r_T is the correlation coefficient computed for the entire line. KT = Kinki Triangle, ISTL = Itoigawa-Shizuoka Tectonic Line, TTL = Tanakura Tectonic Line, and HTL = Hatagawa Tectonic Line.

correlation varies considerably throughout Honshu (Figs. 16C and 17). The appearance of negative area strain in the densely faulted areas of the Kinki Triangle and central Japan Alps between the Kinki Triangle and the ISTL is expected in areas experiencing significant shortening strain and is consistent with convergence between the Eurasian and North American plates currently taking place in central Japan and the Kinki Triangle. That the Kinki Triangle area is currently undergoing vertical as well as horizontal displacements is suggested by recent movements along the MTL and its branching faults (YOKOKURA, 1999; OKADA, 1980).

The lower correlation between 110-year area strain and D_{AF} ($\langle r \rangle = -0.26$) for all three lines (Table 1) appears to arise in part because the region of negative area strain extends farther into southwest Japan (compare Figs. 16 and 18). The correlation

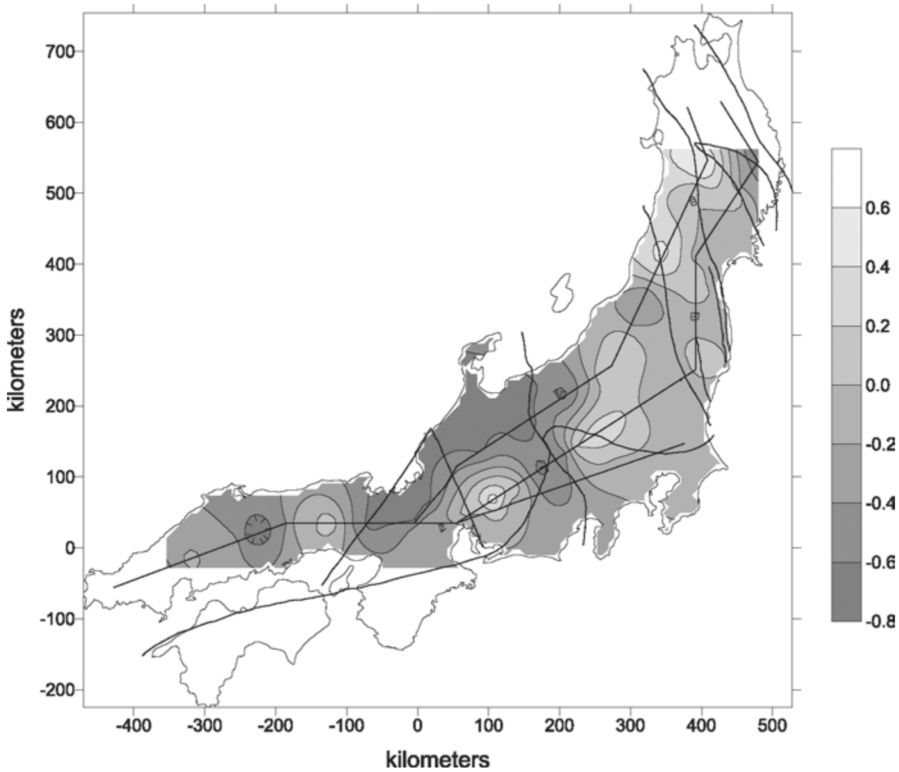

Figure 17
Contours of the local correlation coefficients (r_{ASAF}) between the 10-year area strain and fractal dimension of the active fault complex (D_{AF}).

between D_{AF} and the 110-year area strain computed for Line 1 (located entirely within west and south-central Japan) is nearly zero because of consistently lower 110-year area strain throughout southwestern Japan. Correlation coefficients computed between the 110-year area strain and D_{AF} for lines 2 and 3 are negative (−0.39 and −0.38, respectively) and similar to those obtained from the 10-year strains (−0.43 and −0.49, respectively).

6. Summary and Conclusions

Fractal characterization of complex variables, such as active fault networks and elevation, by their fractal dimension allows us to examine the relationship of fault distribution, and topographic roughness to scalar and vector variables such as Quaternary vertical displacement, crustal strain, and elevation variation over scales of approximately 110 km to 1000 km. This approach is used to evaluate regional

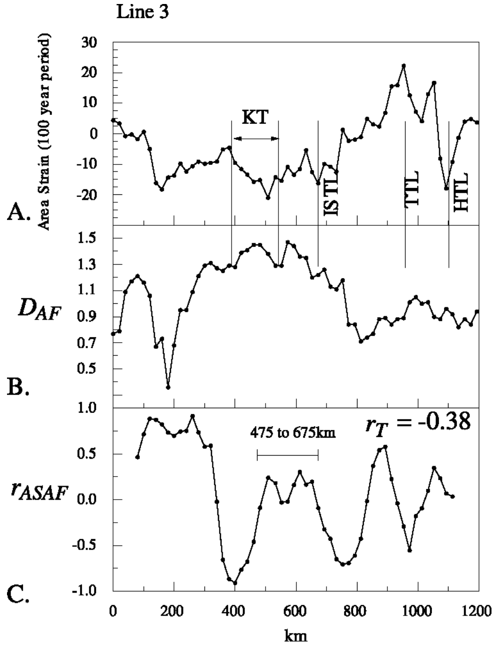

Figure 18
A) The 100-year area strain ($\times 10^{-6}$) along Line 3; B) variations in the fractal dimension of active faults (D_{AF}) computed along Line 3; C) variations in local correlation coefficients (r_{ASAF}) between 100-year area strain and D_{AF}. r_T is the correlation coefficient computed for the entire line. KT = Kinki Triangle, ISTL = Itoigawa-Shizuoka Tectonic Line, TTL = Tanakura Tectonic Line, and HTL = Hatagawa Tectonic Line.

scale correlation between data sets and to identify and map local variability in the correlation between data sets.

Regional correlations between variables summarized in Table 1 reveal similarity ($\langle r \rangle = 0.75$) between Quaternary vertical displacement (QVD) and elevation variation, and QVD and the fractal dimension of topography (D_T). The correlation suggests that QVD has direct influence on present-day elevation variation throughout Japan and on the roughness (or fractal properties) of the topographic surface; areas of large uplift are associated with areas of high elevation and higher surface roughness (D_T). On the other hand, elevation (T), the fractal properties of elevation (D_T), and QVD do not correlate with short-term horizontal crustal strains measured over 10- and 110-year time periods. Short-term horizontal crustal strain must have varied considerably over the 2.5 million-year time frame of the Quaternary so that at any particular instant in time, short-term strain patterns differ from the net long-term strain. The low 0.48 correlation between short-term area strains over 10- and 110-year time intervals and the zero-correlation between maximum shear strains measured over 10- and 110- year time periods highlight that crustal strain changes considerably over these short time frames. Rapid variability in strain rates is also suggested by recent GPS derived strain data during the 1997-1999 time period (Sagiya *et al.*, 2000). The GPS observations of dilatation rate during that time period are entirely contractional.

Short-term strains represented by 10- and 110-year horizontal area strains correlate negatively with the fractal properties of the active fault complex (D_{AF}). The average negative correlation suggests that, in general; more intensely faulted areas (areas of higher D_{AF}) are associated with areas undergoing regional scale negative compressive strain. Negative area strain is in general concentrated in areas west of the Itoigawa-Shizuoka Tectonic Line, which includes areas of greater complexity in the active fault system of Japan. The maps of active faults in Japan published by the Research Group For Active Faults Of Japan (1991) represent only those faults along which displacement occurred sometime during the Quaternary. While central Japan is a region in which the active faults are most complex and in which Quaternary vertical displacements are among the highest throughout Honshu, the fractal properties of the active fault distribution do not correlate well with QVD. Neither do they correlate with elevation (T) or D_T. This result is attributed to the fact that areas of extensive Quaternary vertical displacement, high elevation, and high D_T extending east across the ISTL into the northern Fossa Magna and to less extent into the southern Fossa Magna, are not accompanied by complex fault systems exposed at the surface. On the other hand, the complexly faulted eastern Kinki Triangle region is associated with lesser amounts of vertical uplift, and relatively low elevation and fractal dimension.

Local variability in the correlation between data sets yields insight into short-term tectonic behavior, which in turn may have some bearing on future earthquake hazard assessment. For example, the correlation between area strain and the fractal distribution of active faults along Line 3 for 10- and 110-year time intervals (see Fig. 17 for the 10-year time period) reveals significant change in correlation over those time periods through the densely faulted region of central Japan. Over the 110-year time period, the correlation between D_{AF} and area strain is approximately 0 from 475 and 675 km along Line 3 (see Fig. 18C). However during the recent 10-year time frame this correlation drops to an average of approximately -0.6 through the area (see Fig. 16C). This drop is associated with a shift of maximum negative area strain farther west into the Kinki Triangle. In addition, area strain west of the ISTL begins to rise more steeply into the region of positive shear strain, which is characteristic of northern Japan. Area strains also increase more steeply to the positive in the area southwest of the Kinki Triangle. The implications of this redistribution of strain through the active fault complex may have earthquake hazard significance. The Kinki triangle is an area where maximum earthquake magnitudes are higher than in surrounding areas (generally M 7 and greater (see Oncel *et al.* (2001), their Figure 10)). At this point, our observations are largely phenomenological; the relation of strain variation to the regional distribution of maximum earthquake magnitude and Gutenberg-Richter b value and the tectonic significance of these relationships are part of an ongoing study (see ONCEL and WILSON, 2002). Tectonic relationships are implied by the shifting distribution of area strain within the active fault complex. Positive correlation of the fractal properties of topography and topographic relief with Quaternary vertical displacement are clearly related to the tectonic forces that drive vertical uplift. The presence of high positive correlation through central Japan and into the Fossa Magna results from the convergence of four tectonic plates focused in these areas. The method of analysis presented here and in ONCEL *et al.* (2001) allows us to quantify the interrelationships between complex fractal systems and associated scalar quantities such as elevation and Quaternary Vertical Displacement. Further study of the local variability in the correlation between these variables may yield further insights into local tectonic processes.

Acknowledgements

Comments of anonymous reviewers greatly improved the manuscript. In addition, the comments and suggestions of Shintaro Yagi and Kumaki Yohta of the Geographical Survey Institute of Japan and Jaime Toro (West Virginia University) were very helpful and greatly appreciated. This research was supported through a Japan Science and Technology Agency fellowship hosted through the Geological Survey of Japan. Special thanks to Debbie Benson for her assistance in drafting some of the figures in this paper.

REFERENCES

DOUDS, A. B. (1998), *Fractal Analysis of Topography and Structure across the Appalachian Foreland of West Virginia*, West Virginia University, Masters Thesis, 119 pp.

FEDER, J. (1988), *Fractals* (Plenum Press), 283 pp.

FOX, C. (1989), *Empirically Derived Relationships between Fractal Dimensions and Power Law Form from Frequency Spectra*, Pure Applied Geophys. *131*, 211–239.

GEOGRAPHICAL SURVEY INSTITUTE (1997a), *250 Meter Mesh: Digital Map 250 m Grid (Elevation)*, Geographical Survey Institute, Tsukuba, Japan, or Sales Agency Japan Map Center, Tokyo, Japan, CD-ROM.

GEOGRAPHICAL SURVEY INSTITUTE (1997b), *Horizontal Crustal Strain Map, 1:2,000,000*, Geographical Survey Institute of Japan, Tsukuba, Ibaraki Prefecture, http://cais.gsi.go.jp/HIZUMI/hizumi7.html.

HIRATA, T. (1989), *Fractal Dimension of Fault Systems in Japan: Fractal Structure in Rock Fracture Geometry at Various Scales*, Pure Appl. Geophys. *131*, 157–170.

IKAMI, A., YOSHII, T., KUBOTA, S., SASAKI, Y., HASEMI, A., MORIYA, T., MIYAMACHI, H., MATSU'URA, R., and WADA, K. (1986), *A Seismic Refraction Profile in and around Nagano Prefecture, Central Japan*, J. Phys. Earth *34*, 457–474.

ISHIKAWA, N., TADA, T., and HASHIMOTO, M. (1998), *Horizontal Strain in Japanese Islands, Kokudochirin-Jiho* (Geographical Survey Institute Journal) *89*, 18–26 (in Japanese).

ISOZAKI, Y. (1996), *Anatomy and Genesis of a Subduction Related Orogen: A New View of Geotectonic Subdivision and Evolution of the Japanese Islands*, The Island Arc *5*, 289–320.

JOLIVET, L. and TAMAKI, K. (1994), *Japan Sea, Opening History and Mechanism*: *A synopsis*, J. Geophys. Res. *99*, 22,237–22,259.

KANO, K. and WAKITA, K. (1992), *A Geological Synthesis of the Japanese Islands*: 29th International Geological Congress, Kyoto, Presentation and Abstracts with Programs, 8983.

KANO, K., I. KOSAKA, K., MURATA, A., and YANAI, S. (1990), *Intra-arc Deformations with Vertical Rotation Axes: the Case of the Pre-Middle Miocene Terranes of Southwest Japan*, Tectonophys. *176*, 333–354.

KLINKENBERG, B. and GOODCHILD, M. (1992), *The Fractal Properties of Topography: A Comparison of Methods*, Earth Surface Proc. and Landforms *17*, 217–234.

KOBAYASHI, Y. (1983), *On the Initiation of the Subduction of Plates*, Earth Monthly *5*, 510–514 (in Japanese).

MALINVERNO, A. (1990), *A Simple Method to Estimate the Fractal Dimension of Self-affine Series*, Geophys. Res. Lett. *17*, 1953–1956.

MANDELBROT, B. B. (1967), *How Long is the Coast of Britain? Statistical Self-similarity and Fractional Dimension*, Science *156*, 636–638.

MARESCHAL, J. (1989), *Fractal Reconstruction of Sea-floor Topography*, Pure Appl. Geophys. *131*, 197–210.

MARK, D. and ARONSON, P. (1984), *Scale-dependent Fractal Dimensions of Topographic Surfaces: An Empirical Investigation, with Applications in Geomorphology and Computer Mapping*, Mathemat. Geology *16*, 671–683.

MATSUSHITA, M. and OUCHI, S. (1989), *On the Self-affinity of Various Curves*, Physica D *38*, 246–251.

NAKAMURA, K. (1983), *Possible Nascent Trench along the Japan Sea as the Convergent Boundary between the Eurasian and North American Plates*, Bull. Earthq. Res. Institute *58*, 711–722.

OKADA, A. (1980), *Quaternary Faulting along the Median Tectonic Line of Southwest Japan*, Mem. Geolog. Soc. Japan *18*, 79–108.

OKUMURA, K., SHIMOKAWA, K., YAMAZAKI, H., and TSUKUDA, E. (1994), *Recent Surface Faulting Events along the Middle Section of the Itoigawa-Shizuoka Tectonic Line - Trench Survey of the Gofukuji Fault near Matsumoto, Central Japan*, Zisin *(The Journal of the Seismological Society of Japan)*, *2*, 46, 425–438 (in Japanese with English Abstract).

OKUMURA, K. (2001), *Paleoseismology of the Itoigawa-Shizuoka Tectonic Line in Central Japan*, J. Seismology *5*, 411–431.

ONCEL, A. O., WILSON, T. H., and NISHIZAWA, O. (2001), *Size Scaling Relationships in the Active Fault Networks of Japan and their Correlation with Gutenberg-Richter b Values*, J. Geophys. Res. *106*, B10, 21,827–21,841.

ONCEL, A. O. and WILSON, T. H. (2002), *Space-time Correlations of Seismotectonic Parameters: Examples from Japan and from Turkey Preceding the Izmit Earthquake*, Bull. Seismol. Soc. Am. *92*, 339–349.

PHILLIPS, R. J., ZUBER, M., SOLOMON, S., GOLOMBEK, B., JAKOSKY, B., BARNERDT, W., SMITH, D., WILLIAMS, R., HYNEK, B., AHARONSON, O., and HAUCK, S. (2001), *Ancient Geodynamics and Global-scale Hydrology on Mars*, Science *291*, 2587–2591.

RESEARCH GROUP FOR ACTIVE FAULTS OF JAPAN (1991), *Active Faults in Japan*: *Sheet Maps and Inventories*, (in Japanese), revised edition, University of Tokyo Press, Tokyo, Japan.

RESEARCH GROUP FOR QUATERNARY TECTONIC MAP, TOKYO (1973), *Explanatory Text of the Quaternary Tectonic Map of Japan*: *National Research Center for Disaster Prevention, Science and Technology Agency*, Tokyo, Japan, 167 pp, 3 Plates.

SAGIYA, T., MIYAZAKI, S., and TADA, T. (2000), *Continuous GPS Array and Present-day Crustal Deformation of Japan*, Pure Appl. Geophys. *157*, 2303–2322.

SHIMOKAWA, K. (1997), *Research on Earthquake Potential Assessment around the Eastern Margin of the Japan Sea*, Geological Survey of Japan Information Sheet *S-4*, 4 pp.

SCHOLZ, C. H., *Fractal transitions on geological surfaces*. In *Fractals in the Earth Sciences* (eds. C. C. Barton and P. LaPointe) (Plenum Press, New York, 1995), pp. 131–140.

SUGIMURA, A. and UYEDA, S., *Island Arcs – Japan and its Environs*, Elsevier Scientific Publ. Comp. Develop. Geotect. *3*, (Amsterdam 1973), 247 pp.

TAKAHASHI, M. and NOMURA, S. (1989), *Paleomagnetism of the Chichibu Quartz Diorite – Constraints on the Time of Lateral Bending of the Kanto Syntaxis*, J. Geomagn. and Geoelectricity *41*, 479–489.

TAKAHASHI, M. and SAITO, K. (1997), *Miocene Intra-arc Bending at an Arc-arc Collision Zone, Central Japan*, The Island Arc *6*, 168–182.

TAMAKI, K. (1988), *Geological Structures of the Japan Sea and its Tectonic Implications*, Bull. Geolog. Survey of Japan *39*, 269–365.

TODA, S., KATOH, S., KOBAYASHI, F., KAGAWA, T., YOKOTA, H., NAKAGAWA, K., TAKAMURA, K., and OKADA, A. (1998), *Seismic Reflection Survey across the Central Part of the Arima-Takatsuki Tectonic Line, Kinki District, Central Japan*, Nature and Human Activities *3*, 9–21.

TSUKUDA, E. (1992), *Active Tectonics of Southwest Japan Arc Controlled by the Westward Translation of the Forearc Sliver*, Mem. Geolog. Soc. Japan *40*, 235–250 (in Japanese with English abstract).

TURCOTTE, D. L., *Fractals and Chaos in Geology and Geophysics* (Cambridge University Press, Cambridge 1989), 221 pp.

TURCOTTE, D. L., *Fractals and Chaos in Geology and Geophysics* (Cambridge University Press 1992), 2nd ed., Cambridge, 386 pp.

WAKITA, K. (1997), *The Geology of Japan: A Guide for the CD-Rom "Digital Geologic Map of East and Southeast Asia"*, CCOP Techn. Bull. *26*, 47–57.

WILSON, T. and KATO, H. (1992), *Interpretation of the Matsumoto Basin gravity low*. In Bull. Geolog. Survey of Japan. Special Issue–Cenozoic Geohistory and Tectonics in Japan *43*, nos. (1/2), 31–42.

WILSON, T. and KATO, H. (1995), *Gravity Model Studies of the Northern Fossa Magna: Central Honshu, Japan*, Bull. Geolog. Survey of Japan, *46*, no.(1), 1–22.

WILSON, T. H. and DOMINIC, J. (1998), *Fractal Interrelationships between Topography and Structure*, Earth Surface Processes and Landforms *23*, 509–525.

WILSON, T. H. (2000), *Some Distinctions between Self-similar and Self-affine Estimates of Fractal Dimension with Case History*, Mathem. Geology *32*, 319–335.

WILSON, T. H. (2001), *Scale Transitions in Fracture and Active Fault Networks*, Mathem. Geology *33*, 591–613.

YOKOKURA, T. (1999), *Seismic Investigation of an Active Fault off Kobe: Another Disaster in the Making*, Leading Edge *16*, 1417–1421.

(Received August 15, 2001, accepted July 8, 2002)